

1 **Microcircuit formation following transplantation of mouse embryonic stem cell-**
2 **derived neurons into peripheral nerve**

3
4 Philippe Magown^{1,2}, Victor F. Rafuse^{1,3}, Robert M. Brownstone^{1,2,4}

5
6 ¹Medical Neuroscience, Dalhousie University, Halifax, Nova Scotia, Canada

7 ²Department of Surgery (Neurosurgery), Dalhousie University, Halifax, Nova Scotia,
8 Canada

9 ³Department of Medicine (Neurology), Dalhousie University, Halifax, Nova Scotia,
10 Canada

11 ⁴Sobell Department of Motor Neuroscience and Movement Disorders, Institute of
12 Neurology, University College London, London, UK

13
14 **RUNNING HEAD: Spontaneous activity in ESCMN transplants**

15
16 **CORRESPONDING AUTHORS:**

17 Victor F Rafuse

18 Department of Medical Neuroscience

19 Dalhousie University

20 Halifax, NS

21 Canada

22
23 **OR**

24
25 Robert M. Brownstone

26 Sobell Department of Motor Neuroscience and Movement Disorders

27 University College London Institute of Neurology

28 Queen Square

29 London, UK

30 WC1N 3BG

31 r.brownstone@ucl.ac.uk

32
33 phone: +44 20 3108 9649

34
35 **NEW AND NOTEWORTHY:**

36 This manuscript demonstrates that following peripheral transplantation of neurons
37 derived from embryonic stem cells, the grafts are spontaneously active. The activity is
38 produced and modulated by a number of transmitter systems, indicating that there is a
39 degree of self-assembly of circuits.

40
41 **KEYWORDS:**

42 Peripheral nerve injury

43 Locomotion

44 Central pattern generator

45
46 **AUTHOR CONTRIBUTIONS**

47 PM, VRF, and RMB contributed to the conception and design of the study, PM acquired
48 and analyzed the data, and PM, VRF, and RMB wrote the manuscript.

49 **Abstract**

50 Motoneurons derived from embryonic stem cells can be transplanted into the tibial nerve,
51 where they extend axons to functionally innervate target muscle. Here, we studied
52 spontaneous muscle contractions in these grafts three months following transplantation.
53 One-half of the transplanted grafts generated rhythmic muscle contractions of variable
54 patterns, either spontaneously or in response to brief electrical stimulation. Activity
55 generated by transplanted embryonic stem cell-derived neurons was driven by glutamate
56 and was modulated by muscarinic and GABAergic/glycinergic transmission.
57 Furthermore, rhythmicity was promoted by the same transmitter combination that evokes
58 rhythmic locomotor activity in spinal cord circuits. These results demonstrate that there is
59 a degree of self-assembly of microcircuits in these peripheral grafts involving embryonic
60 stem cell-derived motoneurons and interneurons. Such spontaneous activity is
61 reminiscent of embryonic circuit development in which spontaneous activity is essential
62 for proper connectivity and function, and may be necessary for the grafts to form
63 functional connections with muscle.

64 **Introduction**

65 Spontaneous activity of neurons during embryogenesis is important for the development
66 of neural circuits (Kirkby et al., 2013). Such activity plays a role in synapse development
67 as well as axon path-finding (Gomez and Spitzer, 1999; Hanson and Landmesser,
68 2004). In early embryogenesis of the spinal cord, release of acetylcholine from
69 developing motoneurons (MNs) has been shown to be crucial for the development of
70 locomotor circuits (Myers et al., 2005). This is a transient requirement, as later in
71 development eliminating cholinergic neurotransmission has little effect (Myers et al.,
72 2005), and glutamate and glycine/GABA release from interneurons plays an increasing
73 role in bursting behaviour (Rosato-Siri et al., 2004). Thus, various neuronal populations
74 and various transmitter phenotypes play different roles in spontaneous bursting activity
75 at different time points in development, and this activity is essential for the development
76 of synapses and circuits.

77 Motoneurons can be derived in vitro from embryonic stem cells through exogenous
78 application of signalling factors present in the ventral spinal cord during development
79 (Wichterle et al., 2002). Although this results in enrichment of MNs in these cultures
80 (Wichterle et al., 2002; Miles et al., 2004), a wide range of neuronal subtypes remains:
81 the typical MN differentiation protocol generates about 30% MNs as well as different
82 interneuron types: glutamatergic (10%), GABAergic (15%), and glycinergic (6%)
83 (Deshpande et al., 2006). Some of these neurons express markers associated with
84 specific excitatory or inhibitory ventral spinal interneuronal types (Deshpande et al.,
85 2006). Embryonic stem cell derived motoneurons (ESCMNs) can functionally innervate
86 muscle in culture (Miles et al., 2004; Chipman et al., 2014), or following transplantation
87 into either developing chick embryos (Soundararajan *et al.*, 2006) or adult mouse

88 peripheral nerve (Yohn et al., 2008; Bryson et al., 2014; Magown et al., 2016), but we
89 and others have had less success when transplanting purified ESCMNs. It is possible
90 that neurons other than MNs facilitate neuromuscular innervation, possibly through
91 inducing activity. In fact, spontaneous activity has been demonstrated in vitro in neurons
92 derived from stem or pluripotent cells (Ban et al., 2007; Heikkilä et al., 2009; Illes et al.,
93 2014), but whether such activity is present following transplantation or involved in
94 innervation is not known.

95 We therefore asked whether there is evidence of circuit formation and spontaneous
96 activity in ESCMNs transplanted into adult mouse peripheral nerve, isolated from the
97 central nervous system. Our previously used model whereby neurons are implanted into
98 the peripheral nervous system (Thomas et al., 2000; Yohn et al., 2008) avoids the
99 growth-inhibiting environment of the central nervous system. Furthermore, this strategy
100 ensures that all innervation following transplantation is attributable to transplanted rather
101 than endogenous MNs. Using this peripheral nerve transplantation model, we previously
102 reported spontaneous EMG activity in transplanted animals, but had thought this might
103 be secondary to mechanical stimulation (Yohn et al., 2008). Here we extended these
104 studies to characterize spontaneous circuit activity in these transplants, and found that
105 they exhibited spontaneous and stimulation-evoked rhythmic muscle contractions. This
106 activity was glutamate-dependent, suggesting formation of circuits with excitatory
107 interneurons. Furthermore, GABA/glycine and acetylcholine activity modulated the circuit
108 function. We conclude that after transplantation, a self-organized circuitry forms that is
109 capable of driving rhythmic muscle contraction.

110 **Methods**

111 **Embryonic Stem Cell Derived Motoneurons**

112 Generation of mouse embryonic stem cell derived MNs has been previously described
113 (Wichterle et al., 2002; Miles et al., 2004; Yohn et al., 2008). In summary, HBGB6 mouse
114 stem cells expressing GFP under the motoneuronal promoter Hb9 (Magown et al., 2016)
115 were agglomerated as embryonic bodies before differentiation with smoothen agonist
116 (500 nM, Enzo) and retinoic acid (1 μ M, Sigma) for 5 days. The presence of MNs was
117 confirmed by the expression of GFP.

118 **ESCMN Transplantation**

119 All procedures were performed in accordance with protocols approved by the Dalhousie
120 University Animal Care Committee, and conformed to the standards of the Canadian
121 Council of Animal Care. Details of the ESCMN dissociation and transplantation can be
122 found in a previous publication (Yohn et al., 2008; Magown et al., 2016). In summary,
123 embryonic bodies were treated with 1 μ g/ml mitomycin C (except for immediate
124 transplants) for 2 hours followed by wash, dissociation and resuspension at 10^6 cells per
125 10 μ L of DFK10 with 10 μ g/ml GDNF (Milipore), 20 μ g/ml CNTF (Chemicon) and 0.01%
126 DNaseI (Sigma-Aldrich).

127 Transplantation was performed in 5 week-old mice either immediately after nerve
128 transection or after a delay of 1, 2 or 4 weeks post transection as previously described
129 (Magown et al., 2016). Briefly, the tibial nerve was transected proximal to the branching
130 of the nerve to the medial gastrocnemius (MG). The proximal tibial nerve stump was
131 ligated and buried into the adjacent muscle to prevent reinnervation. Ten thousand cells
132 in 0.1 μ L were transplanted in the distal tibial nerve with a glass pipette.

133 ***In Vitro* Electrophysiological Recordings**

134 The MG muscle and the transplanted tibial nerve were harvested 3 months post
135 transplantation and maintained in an *in vitro* chamber circulating oxygenated mouse
136 Tyrode's solution (125 mM NaCl, 24 mM NaHCO₃, 5.4 mM KCl, 1 mM MgCl₂, 1.8 mM
137 CaCl₂, and 5% dextrose) at room temperature (Yohn et al., 2008). Stimulation to evoke
138 bursting activity was provided to the MG nerve with a suction electrode via a square
139 pulse stimulator (S88, Grass Technologies) and a stimulus isolation unit (PSIU6, Grass
140 Technologies) at 1.5x the maximal stimulus threshold (usually ~10 V, 100 μ A). Three
141 pulses of 0.2 ms at 5 Hz or 25 pulses at 50 Hz were used to elicit bursting activity.
142 Forces were measured with a force transducer (FT03, Grass Technologies) connected to
143 a strain gage amplifier (P122, Grass Technologies). Signals were recorded via a
144 Digidata 1320A, using Axoscope 9.2 software (Molecular Devices). Forces were
145 analyzed off-line. Bursts were detected using event analysis in pClamp 10 (Molecular
146 Devices) using threshold detection set with a minimal amplitude of 0.5 mN (2 standard
147 deviation above baseline noise recorded after nerve transection) and a minimum
148 duration of 50 ms.

149 The following drugs were used: CNQX 10 μ M (disodium salt hydrate, #115066-14-3,
150 Sigma), APV 100 μ M (#76326-31-3, Sigma), bicuculline 10 μ M (#485-49-4, Sigma),
151 strychnine hydrochloride 1 μ M (#1421-86-9, Sigma), atropine 10 μ M (51-58-8, Sigma),
152 NMDA 5 μ M (#6384-92-5, Sigma), serotonin hydrochloride (5-HT) 10 μ M (#153-98-0,
153 Sigma) and dopamine hydrochloride 50 μ M (#62-31-7, Sigma). All drugs were added as
154 a concentrated stock to the circulating Tyrode's solution to give the final concentrations
155 indicated above.

156 **Statistical Analysis**

157 Statistical analysis was performed before and after drug infusion on each animal
158 individually. Because of the high variability of responses between animals, results were
159 not combined for analysis and the number of animals is indicating by N. For individual
160 animals, effects of drugs (measuring multiple bursts) were compared to baseline
161 (multiple bursts) using unpaired t-tests with Welch's correction or with a Mann-Whitney
162 test if data groups failed a D'Agostino-Pearson normality test. When more than two
163 groups were compared, a one-way ANOVA test was performed. A Chi-square test was
164 performed when analyzing ratio. Results are presented as means \pm standard deviations.
165 Statistics were performed using GraphPad Prism version 6.0h for Mac (GraphPad
166 Software, La Jolla, California USA).

167 **Results**

168 Motoneurons derived from embryonic stem cells were transplanted into the tibial nerve
169 acutely after transection or after a denervation period of up to four weeks. MG forces
170 were recorded *ex vivo* three months after transplantation (Magown et al., 2016). Out of
171 24 transplanted mice (the same mice as reported in Magown et al., 2016), 17
172 demonstrated contraction of the MG upon electrical stimulation of the transplant site,
173 indicating functional engraftment. Of these 17 mice, 9 (53%) had rhythmic contractions,
174 of which 6 were spontaneously rhythmic in the absence of electrical stimulation (Movie
175 1), and 3 had episodes of repetitive contractions evoked by either a single electrical
176 pulse or a short train of pulses (Figure 1A). Cutting the tibial nerve distal to the transplant
177 resulted in complete ablation of rhythmic contractions in all 9 mice. Using the
178 nomenclature “burst” to indicate a single spontaneously terminating contraction,
179 “bursting” to indicate repetitive bursts, and “episode” to indicate a period of repetitive
180 bursting, transplantation of ESCMNs led to spontaneous or evocable bursting episodes
181 in one-half (9 / 17) of the preparations.

182 To determine the origin of the rhythmic activity, we next investigated the role of
183 glutamatergic transmission in the contractions. Addition of the glutamate receptor
184 blockers CNQX and APV to the preparations with evoked bursting completely prevented
185 further prolonged stimulus-evoked bursting (N = 2; Figure 1A). That is, following
186 glutamate receptor blockade, there was persistence of stimulation-evoked short latency
187 contractions, consistent with our previous findings that following transplantation of these
188 cells, NMJ transmission is cholinergic (Yohn et al., 2008; Magown et al., 2016). In
189 transplants with spontaneous activity, the antagonists eliminated all large amplitude
190 bursts, resulting in a significant reduction in mean amplitudes of burst forces (to 28% and

191 63% of baseline in the two preparations, $p < 0.05$) and a reduction in burst amplitude
192 variance (Figure 1B, C). The remaining low amplitude bursts may reflect single motor
193 units, as the forces recorded (< 4 mN) are similar to motor unit forces following
194 transplantation (Magown et al., 2016). In addition to blocking the large amplitude bursts,
195 glutamate antagonist application also led to a higher frequency of bursting ($N = 2$; Figure
196 1B, C). Autocorrelation analysis revealed no significant burst rhythmicity (Figure 1D).
197 The loss of high amplitude bursts indicates that intrinsic glutamatergic transmission
198 leads to synchronization of MN activity. That is, glutamatergic inputs drive coordinated
199 ESCMN activity.

200 We next asked whether inhibitory inputs contribute to the rhythmicity. In one of two
201 transplants that were spontaneously active, application of combined GABA and glycine
202 antagonists led to a transient increase in force (Figure 1E-G). After 30 minutes without
203 washout, forces returned to baseline (denoted “late” on Figure 1G). No further effect was
204 seen on washout. While there was no change in frequency of the bursts, the activity
205 became more organized over time, as demonstrated by the autocorrelogram (Figure 1H).
206 Thus, GABA/glycine neurotransmission in the transplants limited burst amplitude, and
207 also led to a degree of desynchronization of MN rhythmicity. Given the different time
208 courses of these two effects, the roles of GABA and glycine in burst amplitude and burst
209 synchrony were likely independent of one another with the former effect possibly due to
210 MN inhibition and the latter to desynchronization of activity of the neurons involved in
211 generating the bursting.

212 We next focused on the effects of cholinergic transmission, given the known role of
213 cholinergic activity in the generation of spontaneous activity in embryonic spinal cords
214 (Wenner and O'Donovan, 2001; Myers et al., 2005; Czarnecki et al., 2014; Gonzalez-

215 Islas et al., 2015). As nicotinic blockade would block muscle contraction, we were limited
216 to studying muscarinic responses (N = 3). In the one preparation in which bursting
217 activity was stimulus-evoked, the duration of the episode more than doubled. In
218 transplants with spontaneous activity (N = 2), application of atropine led to an apparent
219 increase in activity (Figure 2A). On closer examination of the baseline data, a
220 background activity of low amplitude bursts (2.7 ± 0.5 mN at 3.4 Hz) could be identified
221 amongst the larger amplitude bursts (17.8 ± 6.6 mN at 1.4 Hz) (Figure 2B), with each of
222 the latter was comprised of multiple contractions (Figure 2A, inset). Following atropine,
223 each large burst was a single contraction, rendering the mean instantaneous frequency
224 of the large bursts lower following atropine. The mean frequency of the low amplitude
225 bursts was also decreased (Figure 2C). Atropine also led to an increase in overall mean
226 burst force amplitudes (Figure 2D) due to the greater proportion of large amplitude
227 events (Figure 2E), but the forces of the low and high amplitude bursts were each
228 unchanged (Figure 2D). Together, these findings suggest that the large amplitude bursts
229 seen after atropine application resulted from summation of multiple small amplitude
230 bursts. In other words, muscarinic activation has several effects. It results in
231 desynchronization of MN firing, which leads to an increase in low amplitude bursts.
232 Furthermore, muscarinic receptor activation leads to high frequency, intermittent MN
233 bursting.

234 Given the above evidence of circuit formation, we asked whether transplanted ESCMNs
235 could sustain rhythmic contractions by adding the neurochemicals that induce locomotor-
236 like rhythmicity in the mouse spinal cord: NMDA, 5-HT and DA (Jiang et al., 1999). The
237 addition of these neurochemicals did not transform transplants with evoked bursting
238 activity (N = 2) into those with spontaneous activity. However, evoked bursting episodes

239 were significantly prolonged (Figure 3A, B). In the transplants that were spontaneously
240 active (N = 2), burst frequency increased (Fig 3C-D). Furthermore, the numbers of bursts
241 greater than 40 mN increased significantly, leading to an overall increase in mean
242 contraction forces (Fig 3E-F). That is, addition of NMDA, 5-HT, and DA resulted in an
243 enhancement of rhythmic motor output, raising the possibility that rhythm-generating
244 elements akin to those in spinal locomotor circuits had formed.

245 **Discussion**

246 We have shown that ESCMNs transplanted into the transected tibial nerve after muscle
247 denervation can generate coordinated rhythmic bursting activity. These bursts are
248 glutamate-dependent and are modulated by GABAergic/glycinergic and cholinergic
249 inputs. Addition of neurochemicals that lead to locomotor activity in the spinal cord,
250 NMDA, 5-HT and DA, promotes bursting episodes, lengthening their duration, increasing
251 contraction forces, and increasing burst frequencies. Together, these data demonstrate
252 that protocols to differentiate ES cells towards MN lineages generate neuronal
253 populations capable of generating rhythmic activity.

254 While these data indicate that there is a degree of self-assembly of microcircuits, the
255 nature and interconnectivity of these circuits is not clear. It is likely that these circuits
256 result from connectivity between a variety of neuronal types. While neuromuscular
257 transmission in this preparation is cholinergic, it is possible that ESCMNs release
258 glutamate locally as they do in the spinal cord (Mentis et al., 2005; Nishimaru et al.,
259 2005; Lamotte d'Incamps and Ascher, 2008), and this glutamate leads to bursting of
260 ESCMNs (MacLean et al., 1997) coordinated by a high degree of MN-MN
261 interconnectivity (chemical and/or electrical; Figure 4A). However this alone does not
262 explain the effects of GABA/glycine, or the differential effects on force amplitudes vs
263 rhythms when adding antagonists. For example, the results show that glutamatergic
264 activity leads to large amplitude forces but no increase in rhythmicity, which would not be
265 expected if the neurons producing the force-regulating output (MNs) were the same as
266 those producing the rhythmicity. Furthermore, if the bursting resulted from MN-MN
267 interactions alone, we would expect acetylcholine to have a synchronizing rather than

268 the desynchronizing effect seen. Thus, the bursting activity likely results from circuits that
269 include interneuron types.

270 It is known that basic elements for the formation of rhythmic motor circuits are present in
271 these cultures. Despite using a differentiation protocol that leads to MN enrichment (Lee
272 et al., 2000; Westmoreland et al., 2001; Barberi et al., 2003; Peljto and Wichterle, 2011),
273 a wide range of neuronal subtypes remains. The typical MN differentiation protocol
274 involves the use of smoothen agonist and retinoic acid (Wichterle et al., 2002), and
275 generates about 30% MNs as well as different interneuron types including glutamatergic,
276 GABAergic, and glycinergic (Deshpande et al., 2006). That is, neuronal types needed for
277 fundamental circuit formation are present. The Sutton principal leads us to suggest that
278 the inter-preparation variability in bursting behavior is explained by differences in the
279 proportions of the neuron types in the transplants. The present neuron types together
280 form an “emerging” circuit capable of generating a rhythm (Figure 4B).

281 **Embryonic Spontaneous Activity**

282 Spontaneous activity is an essential component for the development of embryonic neural
283 circuits (Marder and Rehm, 2005; Blankenship and Feller, 2009) and is involved in
284 various roles, including neurite outgrowth (Metzger et al., 1998), maturation of electrical
285 properties (Xie and Ziskind-Conhaim, 1995), synaptogenesis and axon pathfinding
286 (Hanson and Landmesser, 2004; 2006; Hanson et al., 2008). The roles of different
287 transmitter systems may differ at different times of development. In the early phase of
288 embryonic circuit activity, bursting is dependent on GABAergic and cholinergic
289 transmission, while glutamatergic effects occur at later stages (Branchereau et al., 2002;
290 Hanson and Landmesser, 2003; Myers et al., 2005; Scain et al., 2010). Thus, multiple

291 transmitter systems play different roles in spontaneous activity at different times during
292 development.

293 We studied rhythmic activity at a single time point when such transplants can
294 successfully innervate host muscle (Yohn et al., 2008). The bursting activity we observed
295 was largely glutamate-dependent, corresponding to glutamatergic predominance in late
296 embryonic development. It is possible that earlier following transplantation, there was
297 spontaneous activity produced by other transmitter systems similar to those in early
298 embryogenesis, and that this activity set the stage for circuit formation.

299 Whether spontaneous activity is necessary for successful transplantation is not clear.
300 We and others have observed that transplantation of purified MNs has not been
301 successful. Furthermore, we have shown that following transplantation of non-purified
302 ESCMNs, reinnervation is sub-optimal: force recovery plateaus at 40 to 50%, forces are
303 not always sustained during 50 Hz tetanic stimulation, neuromuscular transmission can
304 decrease with repeated stimulation, and motor unit sizes are smaller than expected for a
305 reinnervated muscle (Yohn et al., 2008). Together, these anomalies point towards
306 defects in maturation of electrical properties, synaptogenesis, axonal pathfinding, and/or
307 neurite outgrowth and sprouting. All of these processes are dependent on MN activity.
308 Thus, we suggest that activity of the transplants facilitates successful reinnervation and
309 improved functional outcomes.

310 **Functional Considerations**

311 Investigating spontaneous activity of ES cell-derived neurons could extend our
312 understanding of developmental neurophysiology and circuit formation (Ban et al., 2007;
313 Heikkilä et al., 2009; Illes et al., 2014). Such knowledge could provide insight into the

314 impacts of transplanted stem cell-derived neurons on host circuits, some of which may
315 be unwanted and of clinical significance, such as uncontrollable contractions
316 (Weerakkody et al., 2013; Illes et al., 2014). Whether the microcircuit formation that
317 resulted in spontaneous activity observed here plays an important role in the functional
318 integration of the transplants, and/or whether it produces clinically undesirable effects
319 remains to be seen.

320 **Acknowledgements**

321 The authors would like to thank Drs Tim Cope, Stefan Krueger, and Jim Fawcett for their
322 input, Cindee Leopold for cell culture support and Angelita Alcos for technical support.

323 PM was supported by a Canadian Institutes of Health Research (CIHR) doctoral
324 fellowship award. This work was funded by the Natural Sciences and Engineering
325 Research Council (VFR), CIHR Neuromuscular Research Partnership (VFR), and CIHR
326 (RMB: FRN 74633). This research was also undertaken, in part, thanks to funding from
327 the Canada Research Chairs program (RMB).

328 **References**

- 329 **Ban J, Bonifazi P, Pinato G, Broccard FD, Studer L, Torre V, Ruaro ME.** Embryonic
330 stem cell-derived neurons form functional networks in vitro. *Stem Cells* 25: 738–749,
331 2007.
- 332 **Barberi T, Klivenyi P, Calingasan NY, Lee H, Kawamata H, Loonam K, Perrier AL,**
333 **Bruses J, Rubio ME, Topf N, Tabar V, Harrison NL, Beal MF, Moore MAS, Studer L.**
334 Neural subtype specification of fertilization and nuclear transfer embryonic stem cells
335 and application in parkinsonian mice. *Nat Biotechnol* 21: 1200–1207, 2003.
- 336 **Blankenship AG, Feller MB.** Mechanisms underlying spontaneous patterned activity in
337 developing neural circuits. *Nat Rev Neurosci* 11: 18–29, 2009.
- 338 **Branchereau P, Chapron J, Meyrand P.** Descending 5-hydroxytryptamine raphe inputs
339 repress the expression of serotonergic neurons and slow the maturation of inhibitory
340 systems in mouse embryonic spinal cord. *Journal of Neuroscience* 22: 2598–2606,
341 2002.
- 342 **Bryson JB, Machado CB, Crossley M, Stevenson D, Bros-Facer V, Burrone J,**
343 **Greensmith L, Lieberam I.** Optical Control of Muscle Function by Transplantation of
344 Stem Cell-Derived Motor Neurons in Mice. *Science* 344: 94–97, 2014.
- 345 **Chipman PH, Zhang Y, Rafuse VF.** A Stem-Cell Based Bioassay to Critically Assess
346 the Pathology of Dysfunctional Neuromuscular Junctions. *PLoS ONE* 9: e91643, 2014.
- 347 **Czarnecki A, Le Corrionc H, Rigato C, Le Bras B, Couraud F, Scain AL, Allain AE,**
348 **Mouffle C, Bullier E, Mangin JM, Branchereau P, Legendre P.** Acetylcholine Controls
349 GABA-, Glutamate-, and Glycine-Dependent Giant Depolarizing Potentials that Govern
350 Spontaneous Motoneuron Activity at the Onset of Synaptogenesis in the Mouse
351 Embryonic Spinal Cord. *J Neurosci* 34: 6389–6404, 2014.
- 352 **Deshpande DM, Kim Y-S, Martinez T, Carmen J, Dike S, Shats I, Rubin LL,**
353 **Drummond J, Krishnan C, Hoke A, Maragakis N, Shefner J, Rothstein JD, Kerr DA.**
354 Recovery from paralysis in adult rats using embryonic stem cells. *Ann Neurol* 60: 32–44,
355 2006.
- 356 **Gomez TM, Spitzer NC.** In vivo regulation of axon extension and pathfinding by growth-
357 cone calcium transients. *Nature* 397: 350–355, 1999.
- 358 **Gonzalez-Islas C, Garcia-Bereguian MA, O'Flaherty B, Wenner P.** Tonic nicotinic
359 transmission enhances spinal GABAergic presynaptic release and the frequency of
360 spontaneous network activity. *Dev Neurobiol* (June 23, 2015). doi: 10.1002/dneu.22315.
- 361 **Hanson MG, Landmesser LT.** Characterization of the circuits that generate
362 spontaneous episodes of activity in the early embryonic mouse spinal cord. *Journal of*
363 *Neuroscience* 23: 587–600, 2003.
- 364 **Hanson MG, Landmesser LT.** Normal patterns of spontaneous activity are required for

- 365 correct motor axon guidance and the expression of specific guidance molecules. *Neuron*
366 43: 687–701, 2004.
- 367 **Hanson MG, Landmesser LT.** Increasing the frequency of spontaneous rhythmic
368 activity disrupts pool-specific axon fasciculation and pathfinding of embryonic spinal
369 motoneurons. *J Neurosci* 26: 12769–12780, 2006.
- 370 **Hanson MG, Milner LD, Landmesser LT.** Spontaneous rhythmic activity in early chick
371 spinal cord influences distinct motor axon pathfinding decisions. *Brain Research*
372 *Reviews* 57: 77–85, 2008.
- 373 **Heikkilä TJ, Ylä-Outinen L, Tanskanen JMA, Lappalainen RS, Skottman H,**
374 **Suuronen R, Mikkonen JE, Hyttinen JAK, Narkilahti S.** Human embryonic stem cell-
375 derived neuronal cells form spontaneously active neuronal networks in vitro. *Exp Neurol*
376 218: 109–116, 2009.
- 377 **Illes S, Jakab M, Beyer F, Gelfert R, Couillard-Despres S, Schnitzler A, Ritter M,**
378 **Aigner L.** Intrinsically Active and Pacemaker Neurons in Pluripotent Stem Cell-Derived
379 Neuronal Populations. *Stem Cell Reports* 2: 323–336, 2014.
- 380 **Jiang Z, Rempel J, Li J, Sawchuk MA, Carlin KP, Brownstone RM.** Development of
381 L-type calcium channels and a nifedipine-sensitive motor activity in the postnatal mouse
382 spinal cord. *Eur J Neurosci* 11: 3481–3487, 1999.
- 383 **Kirkby LA, Sack GS, Firl A, Feller MB.** A role for correlated spontaneous activity in the
384 assembly of neural circuits. *Neuron* 80: 1129–1144, 2013.
- 385 **Lamotte d'Incamps B, Ascher P.** Four excitatory postsynaptic ionotropic receptors
386 coactivated at the motoneuron-Renshaw cell synapse. *Journal of Neuroscience* 28:
387 14121–14131, 2008.
- 388 **Lee S-H, Lumelsky N, Studer L, Auerbach JM, McKay RD.** Efficient generation of
389 midbrain and hindbrain neurons from mouse embryonic stem cells. *Nat Biotechnol* 18:
390 675–679, 2000.
- 391 **MacLean JN, Schmidt BJ, Hochman S.** NMDA receptor activation triggers voltage
392 oscillations, plateau potentials and bursting in neonatal rat lumbar motoneurons in vitro.
393 *Eur J Neurosci* 9: 2702–2711, 1997.
- 394 **Magown P, Brownstone RM, Rafuse VF.** Tumor prevention facilitates delayed
395 transplant of stem cell-derived motoneurons. *Ann Clin Transl Neurol* (July 1, 2016). doi:
396 10.1002/acn3.327.
- 397 **Marder E, Rehm KJ.** Development of central pattern generating circuits. *Curr Opin*
398 *Neurobiol* 15: 86–93, 2005.
- 399 **Mentis GZ, Alvarez FJ, Bonnot A, Richards DS, González-Forero D, Zerda R,**
400 **O'Donovan MJ.** Noncholinergic excitatory actions of motoneurons in the neonatal
401 mammalian spinal cord. *Proc Natl Acad Sci USA* 102: 7344–7349, 2005.

- 402 **Metzger F, Wiese S, Sendtner M.** Effect of glutamate on dendritic growth in embryonic
403 rat motoneurons. *J Neurosci* 18: 1735–1742, 1998.
- 404 **Miles GB, Yohn DC, Wichterle H, Jessell TM, Rafuse VF, Brownstone RM.**
405 Functional properties of motoneurons derived from mouse embryonic stem cells. *Journal*
406 *of Neuroscience* 24: 7848–7858, 2004.
- 407 **Myers CP, Lewcock JW, Hanson MG, Gosgnach S, Aimone JB, Gage FH, Lee K-F,**
408 **Landmesser LT, Pfaff SL.** Cholinergic input is required during embryonic development
409 to mediate proper assembly of spinal locomotor circuits. *Neuron* 46: 37–49, 2005.
- 410 **Nishimaru H, Restrepo CE, Ryge J, Yanagawa Y, Kiehn O.** Mammalian motor
411 neurons corelease glutamate and acetylcholine at central synapses. *Proc Natl Acad Sci*
412 *USA* 102: 5245–5249, 2005.
- 413 **Peljto M, Wichterle H.** Programming embryonic stem cells to neuronal subtypes. *Curr*
414 *Opin Neurobiol* 21: 43–51, 2011.
- 415 **Rosato-Siri MD, Zoccolan D, Furlan F, Ballerini L.** Interneurone bursts are
416 spontaneously associated with muscle contractions only during early phases of mouse
417 spinal network development: a study in organotypic cultures. *Eur J Neurosci* 20: 2697–
418 2710, 2004.
- 419 **Scain A-L, Le Corrionc H, Allain A-E, Muller E, Rigo J-M, Meyrand P, Branchereau**
420 **P, Legendre P.** Glycine release from radial cells modulates the spontaneous activity and
421 its propagation during early spinal cord development. *Journal of Neuroscience* 30: 390–
422 403, 2010.
- 423 **Soundararajan P, Miles GB, Rubin LL, Brownstone RM, Rafuse VF.** Motoneurons
424 derived from embryonic stem cells express transcription factors and develop phenotypes
425 characteristic of medial motor column neurons. *Journal of Neuroscience* 26: 3256–3268,
426 2006.
- 427 **Thomas CK, Erb DE, Grumbles RM, Bunge RP.** Embryonic cord transplants in
428 peripheral nerve restore skeletal muscle function. *J Neurophysiol* 84: 591–595, 2000.
- 429 **Weerakkody TN, Patel TP, Yue C, Takano H, Anderson HC, Meaney DF, Coulter**
430 **DA, Wolfe JH.** Engraftment of nonintegrating neural stem cells differentially perturbs
431 cortical activity in a dose-dependent manner. *Mol Ther* 21: 2258–2267, 2013.
- 432 **Wenner P, O'Donovan MJ.** Mechanisms that initiate spontaneous network activity in the
433 developing chick spinal cord. *J Neurophysiol* 86: 1481–1498, 2001.
- 434 **Westmoreland JJ, Hancock CR, Condie BG.** Neuronal development of embryonic
435 stem cells: a model of GABAergic neuron differentiation. *Biochemical and Biophysical*
436 *Research Communications* 284: 674–680, 2001.
- 437 **Wichterle H, Lieberam I, Porter JA, Jessell TM.** Directed differentiation of embryonic
438 stem cells into motor neurons. *Cell* 110: 385–397, 2002.

- 439 **Xie H, Ziskind-Conhaim L.** Blocking Ca(2+)-dependent synaptic release delays
440 motoneuron differentiation in the rat spinal cord. *J Neurosci* 15: 5900–5911, 1995.
- 441 **Yohn DC, Miles GB, Rafuse VF, Brownstone RM.** Transplanted mouse embryonic
442 stem-cell-derived motoneurons form functional motor units and reduce muscle atrophy.
443 *Journal of Neuroscience* 28: 12409–12418, 2008.
- 444

445 **Figure Legends**

446 **Movie 1 – Spontaneous activity of differentiated ESCs produces rhythmic muscle**
447 **contraction**

448 Ex vivo transplanted tibial nerve under surgical microscope. Enlargement at the end of
449 nerve represents the transplantation site. Top muscle is the medial gastrocnemius
450 spontaneously contracting. Femur is anchored on the left with pins. Suction electrode on
451 top of muscle for EMG recording. Stimulating electrode at the bottom is not contacting
452 the nerve and not stimulating.

453

454 **Figure 1 – Transplanted ESCMNs Generate A Neuronal Circuit Resulting In**
455 **Rhythmic Muscle Contractions**

456 (A) Bursting activity evoked after three 5 Hz stimuli over 500 ms. Evoked activity was
457 blocked after the addition of CNQX and APV (N = 2). Arrows represent electrical stimuli.
458 (B) Spontaneous muscle contractions at baseline, after CNQX and APV infusion, and
459 after washout (N = 2). Spontaneous contractions were significantly reduced after CNQX
460 and APV infusion with residual low amplitude contractions shown in the inset. Grey bars
461 indicate region of insets showing small amplitude bursts in the background. Note the
462 smaller scale bars and truncated events above 5 mN. (C) Quantification of force and
463 instantaneous contraction frequency before and after CNQX and APV. **** One-way
464 ANOVA, $p < 0.0001$. “+” represents mean. (D) Autocorrelation of baseline, CNQX and
465 APV, and washout conditions (N = 1). Dotted lines represent 5% confidence interval. (E-
466 F) Addition of GABA and glycine blockers, bicuculline and strychnine, resulted in an
467 increase in force early, but not late after infusion of GABA and glycine blockers. Grey
468 bars in (E) indicate regions depicted in (F). (G) Quantification of burst amplitude and
469 instantaneous frequency. **** $p < 0.0001$ by one-way ANOVA (N = 1). (H)

470 Autocorrelation of baseline (solid black), early GABA / glycine blockade (dotted grey) and
471 late GABA / glycine blockade (solid grey). Rhythmicity can be seen after prolonged
472 GABA / glycine blockade. Horizontal dotted lines represent 5% confidence interval.

473

474 **Figure 2 – Muscarinic Receptor Blockade Alters Bursting Patterns Produced by**
475 **Transplants**

476 (A) Spontaneous activity at baseline and after addition of atropine. The addition of
477 atropine increased the occurrence of large amplitude bursts. Stars indicate region
478 expanded in inset: note the repetitive large bursts (~2 Hz) at baseline, but single burst
479 following atropine. (B) Enlargement of 10s regions contained within the grey bars in (A)
480 showing a decrease in frequency of small amplitude bursts. Post-drug forces are
481 truncated for illustration. (C) Quantification of instantaneous frequency of bursts.
482 Atropine decreases the overall instantaneous frequency. “+” represents mean. **** p <
483 0.0001, unpaired t-test, N = 1. (D) Quantification of force shows an overall increase in
484 force after the addition of atropine. **** p < 0.0001, unpaired t-test, N = 1. (E) Ratio of
485 large and small events at baseline and after atropine. Chi-square p-value < 0.0001.

486

487 **Figure 3 – Transmitters that Evoke Spinal Locomotion Increase Activity of**
488 **Transplants**

489 (A) The addition of NMDA, 5-HT and DA resulted in an increase activity demonstrated by
490 a prolongation of burst duration in evoked activity. (B) Quantification of episode duration.
491 ** p = 0.004, Mann-Whitney test, 8 vs 4 repeats, N = 1. (C-E) In transplants with
492 spontaneous activity, the addition of NMDA, 5-HT and DA increased the instantaneous
493 frequency and the force of bursts. *** p = 0.0002 in (D) and p = 0.0004 in (E), unpaired t-

494 test with Welch's correction, $N = 1$. (F) Frequency histogram of burst amplitude at
495 baseline and after addition of NMDA, 5HT and dopamine.

496

497 **Figure 4 – Potential Schematics of Transplant Circuits**

498 (A) Bursting is produced by a subset of neurons within the transplant, possibly primarily
499 by MN-MN interactions. The circuit could be composed of an assortment of MNs and
500 interneurons or only MNs. Modulation of the circuit is provided by glutamate,
501 acetylcholine and GABA / glycine. Cholinergic release may be from MN collaterals or
502 cholinergic interneurons. Co-release of glutamate and acetylcholine from MNs is
503 depicted by the red and green boutons. MNs may be electrically coupled. Exogenous
504 NMDA, 5HT, and DA provide a modulatory effect. (B) A rhythmogenic circuit provides
505 glutamatergic inputs to MNs. Modulation of this interneuron circuit is provided by
506 extrinsic or intrinsic glutamate, acetylcholine, and GABA / glycine. Direct modulation by
507 acetylcholine and GABA / glycine onto MNs is also possible. The early effect of GABA /
508 glycine blockade producing an increase in force without a change in burst frequency is
509 shown as direct modulation of MNs. The late effect of GABA / glycine blockade is
510 depicted as acting on the rhythmogenic interneuron circuit. Exogenous NMDA, 5HT and
511 DA provide a modulatory effect. Inter-motoneuron connections (electrical or chemical)
512 could contribute to the activity seen, as could MN collaterals projecting to the
513 rhythmogenic circuit.

514

Figure 1

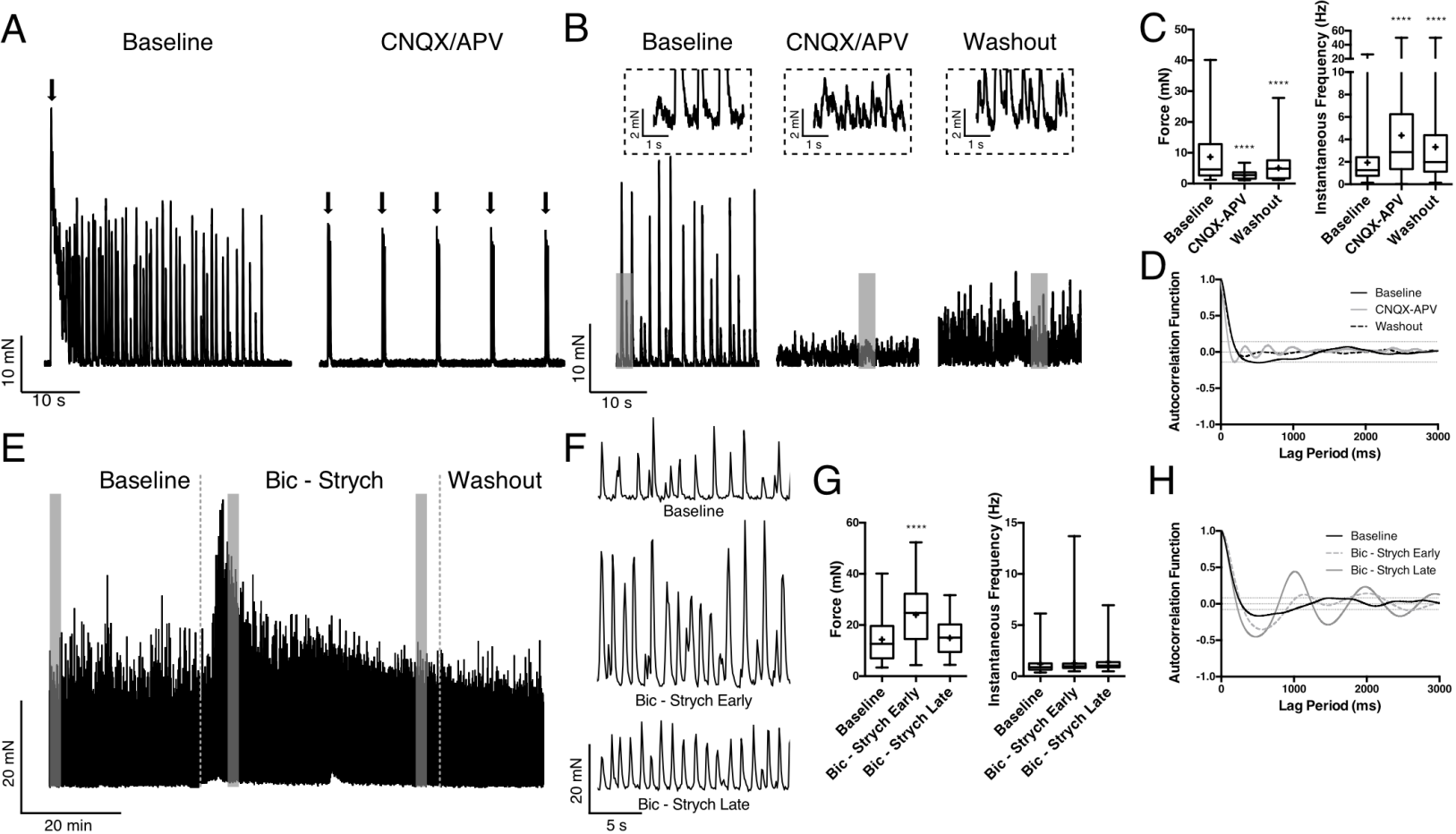


Figure 2

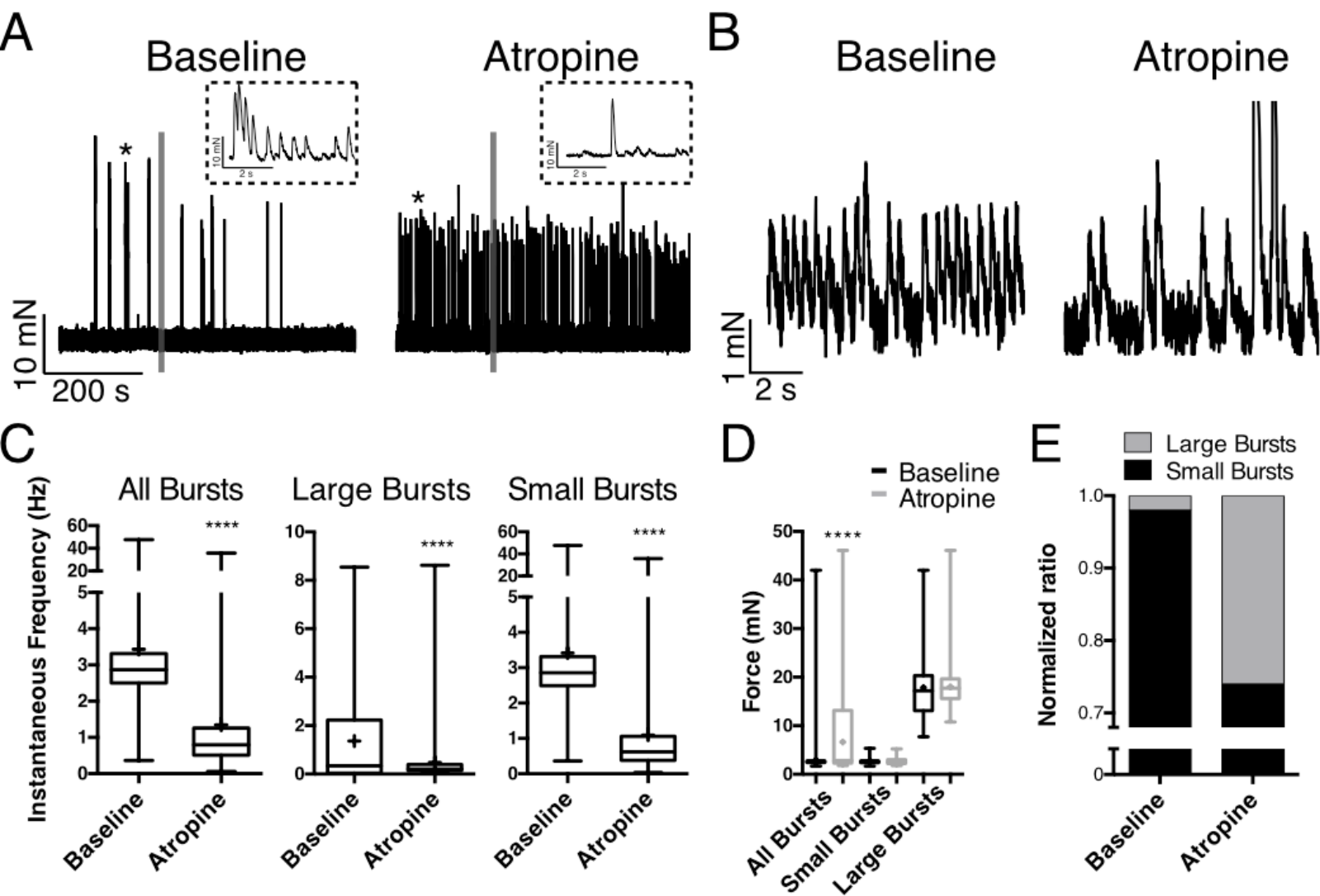


Figure 3

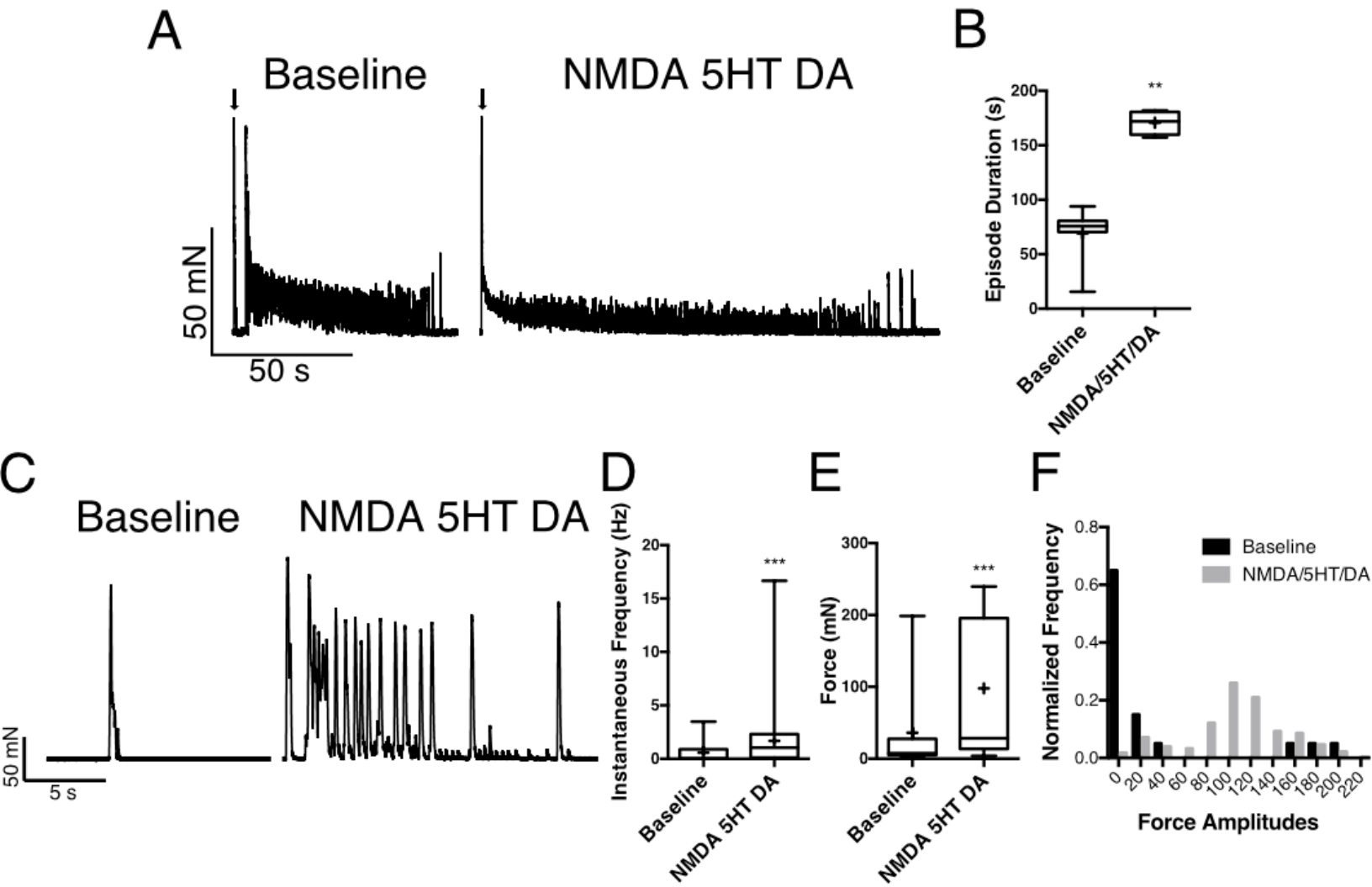
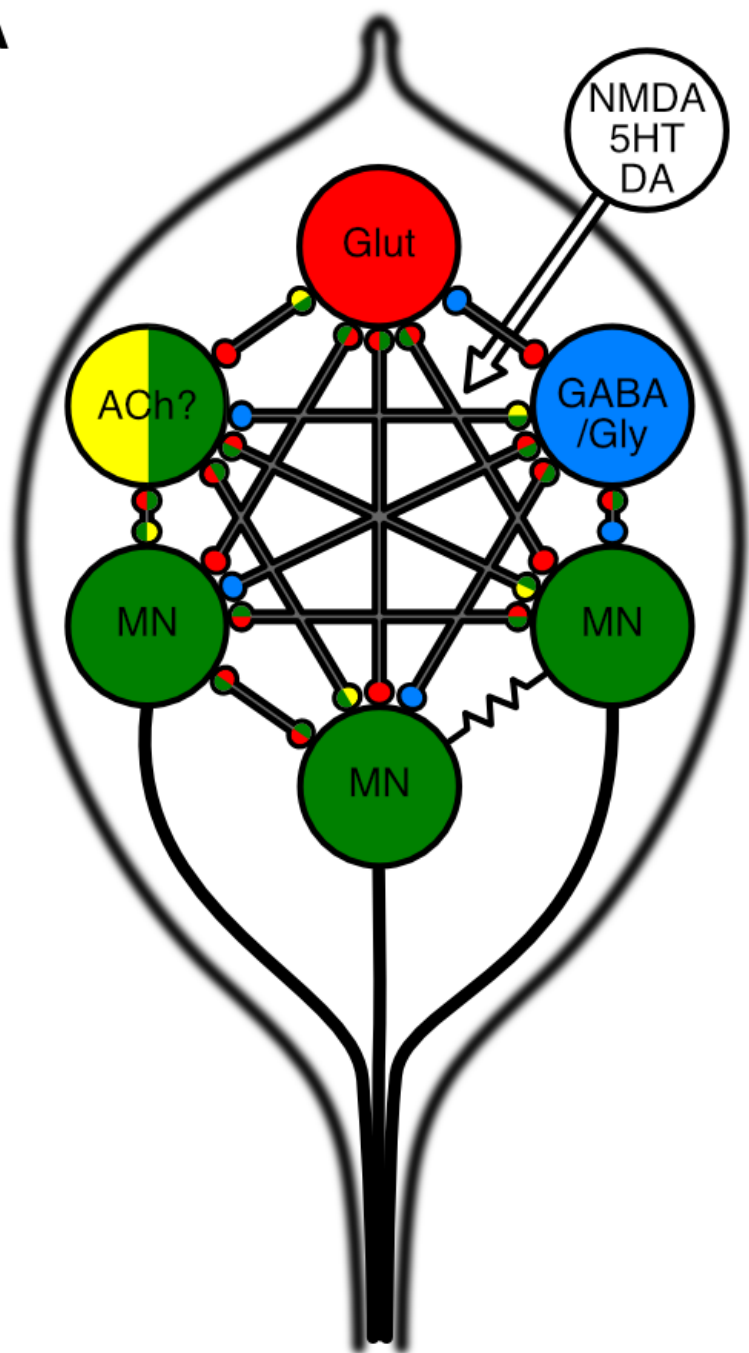


Figure 4

A



B

